Journal of the European Ceramic Society 16 (1996) 759–766

0955-2219(95)00201-4
0955-2219/96/$15.00

The Influence of Crystallization and Washing Medium on the Characteristics of Nanocrystalline Y-TZP

C. D. Sagel-Ransijn, A. J. A. Winnubst, A. J. Burggraaf & H. Verweij

University of Twente, Faculty of Chemical Technology, Laboratory for Inorganic Materials Science, Enschede, The Netherlands

(Received 30 July 1995; revised version received 26 October 1995; accepted 7 November 1995)

Abstract

A zirconia–yttria gel, made by coprecipitation, was treated in six different ways to obtain a nanocrystalline Y-TZP powder: one large gel batch was split into six parts of which one was crystallized in air and the others crystallized either in water with a high pH or in methanol. The batches were subjected to several post treatments. Powder properties and densification characteristics of the six powder batches obtained in this way are described. The air-calcined powder can be sintered to a relative density of about 93% at 1070°C/10 h, but reproducibility of the sintering characteristics is poor. Optimal hydrothermal treatment of the powder yields a reproducible sintering process, resulting in a relative density of 96% at 1070°C/10 h and an average grain size between 120 and 130 nm.

1 Introduction

Nanostructured materials currently receive considerable attention. The percentage of atoms present in the grain boundary region becomes significant once the grain size enters the nanometre regime (i.e. grain size less than 100 nm).[1,2] It is expected that the properties of these nanocrystalline ceramics will be different from those of more conventional materials with phase or grain structures on a coarser scale.[2] He *et al.*[3] have shown that fine-grained zirconia exhibits better wear resistance than the coarse-grained material. For the same material, Theunissen[4] found that both bending strength and fracture toughness at high temperatures are improved with smaller grain sizes. The evaluation of mechanical properties (at low to moderate temperatures) requires the production of bodies with near-theoretical densities. However, preparing bulk materials with near-theoretical densities, while simultaneously keeping the grain size below 100 nm, is not yet possible. The sinterability of the material should permit densification to proceed at such a low temperature that only limited grain growth occurs.

To obtain good sinterability at low temperatures, ultra-fine powders with a low degree of agglomeration are required. The compaction and sintering behaviour of such fine powders is determined, to a large extent, by the strength of their agglomerates. At a given crystallite size, the agglomerate strength can be lowered by increasing the intra-agglomerate porosity and/or decreasing the strength of the interparticle bonds.[5]

Fine powders of ZrO_2 solid solutions can be prepared by a gel precipitation technique using metal chlorides as precursor chemicals.[6,7] This so-called chloride method involves coprecipitation of metal chlorides, followed by water/ammonia and ethanol washing steps. Subjecting the gel to ethanol washing is a crucial step in lowering the strength of the agglomerates. The reduction in strength has been ascribed to the formation of ethoxide groups on the surface[8] and to lower packing density within the agglomerates due to the lower surface tension of ethanol compared with water during the drying process of the powder[9,10] The ethanol washing step doubles the intra-agglomerate porosity after calcination (at 500–550°C) compared with a gel that has been treated with water/ammonia only.[11] The intra-agglomerate porosity of these alcohol-washed powders is sufficiently high to make the agglomerates collapse to a large extent under moderate pressures (50–150 MPa).[7,12] In this way, compacts of uniform pore size distribution are obtained.

Under hydrothermal conditions, crystallization of ZrO_2 solid-solution gels proceeds at temperatures well below 500°C. For example, temperatures of 190–250°C have been reported for the hydrothermal

crystallization of ZrO_2–CaO,[13] ZrO_2–Y_2O_3[14–16] and ZrO_2–CeO_2.[17] Several investigations suggest that the formation of strong interparticle bonds under hydrothermal conditions is greatly diminished or even avoided.[13] Crystallization in organic solvents might be a way to reduce the agglomerate strength even further. Sato *et al.*[17] conclude that crystallization in organic solvents gives better results than hydrothermal crystallization to improve the sinterability, indicating the formation of softer agglomerates in organic solvents. Supercritical drying, which can be performed at a reasonable temperature and pressure for organic solvents, eliminates the effects of capillary forces and might result in even softer agglomerates.

Limited work has been done to address the differences in sinterability of ZrO_2 solid solutions prepared via crystallization in air, hydrothermal crystallization and crystallization in methanol. In the case of ZrO_2–CaO,[13] ZrO_2–CeO_2[17] and ZrO_2–Y_2O_3,[15,16] it has been observed that the sinterability is strongly improved by the hydrothermal treatment. None of these investigations focused on the effect of the washing medium after hydrothermal crystallization. It is expected that this step is important because it affects the surface condition and impurity level of the particles forming the agglomerates.

In this paper, Y-TZP (yttria-stabilized tetragonal zirconia polycrystals) powders are prepared from a dried ethanol-washed gel obtained by coprecipitation and crystallization in air, crystallization under hydrothermal conditions or methanol crystallization. After hydrothermal crystallization, a part of the powder is washed with ethanol. The influence of crystallization medium and post-hydrothermal crystallization treatments on powder properties, green compact structure and sinterability is examined and the synthesis route leading to dense, nanostructured Y-TZP is reported.

2 Experimental Procedure

2.1 Powder synthesis

Appropriate amounts of $ZrCl_4$ (>98% pure) and YCl_3 (99·9% pure) for the preparation of TZP with 5 at% Y on the Zr-site were dissolved in a 0·2 M aqueous HCl solution. The solution was filtered and added drop-wise to an excess of a 25 wt% ammonia solution, with the pH maintained at a value >11. A precipitated gel was obtained and allowed to settle overnight, after which the clear supernatant was removed. The gel obtained was washed with water/ammonia mixtures until the washing liquid no longer became turbid on addition of 0·1 M $AgNO_3$. This indicated that the washing liquid was chloride-free. The gel was subsequently filtered, redispersed and washed twice in ethanol. After drying at 120°C, the gel was divided into four parts as follows.

Table 1. Explanation of codes used

Code	*Explanation*
AC	Air-crystallized
HC	Hydrothermally crystallized
MC	Methanol-crystallized
W	Water-washed
E	Ethanol-washed
SD	Supercritical drying
400	Finally heat-treated at 400°C

(1) The first part was dry milled, calcined in static air at 500°C for 2 h and dry milled again (AC500) (explanation of codes is given in Table 1).

(2) The second part was used for hydrothermal crystallization in a stainless steel autoclave equipped with poly(tetrafluoroethylene) liner. Crystallization of the gel took place at 200°C for 2 h in a basic medium (ammonia solution) at a pressure of 20–30 bar. After hydrothermal treatment, the pH of the slurry was 9–11. The slurry was divided into three parts:
   (a) one part was filtered, dried at 120°C and dry milled (HC-W);
   (b) the second part was treated as above (HC-W) and additionally heat-treated at 400°C for 1 h (HC-W400);
   (c) the third part was redispersed and washed three times in ethanol, filtered and dried at 120°C. The dried powder was subsequently dry milled and heat-treated at 400°C for 1 h to remove residual organics (HC-E400).

(3) The third part was used for crystallization in methanol. Crystallization took place at 250°C for 2 h at a pressure of 130 bar. The powder was supercritically dried at the same temperature and pressure, dry milled and heat-treated at 400°C for 1 h (MC-SD400).

(4) The fourth part was also used for crystallization in methanol. Crystallization also took place at 250°C for 2 h at a pressure of 130 bar. After crystallization, the powder was washed three times in ethanol, dry milled and heat treated for 1 h at 400°C (MC-E400).

In all cases, dry milling was performed with zirconia balls.

For the above-mentioned syntheses, the effects of crystallization medium and post-hydrothermal crystallization treatments (washing, drying and/or temperature treatment) on powder and sintering characteristics were researched.

2.2 Green compact formation and sintering

Green compacts were prepared by cold-isostatic pressing in two steps: initially at 80 MPa and finally at 400 MPa with a 3 min holding time. Sintering was studied by means of dilatometry using a Netzsch 402 E dilatometer. The dilatometer's thermocouple was carefully calibrated by the melting method proposed by Henderson *et al.*[18] Densities were calculated from the green density and the observed linear shrinkage of the specimens, and corrected for thermal expansion and weight loss (due to removal of absorbed water). Final densities calculated in this way were in good agreement with those measured by Archimedes' technique (in Hg). All experiments were performed using cylindrical specimens with initial dimensions 7–15 mm (height) by 6–7 mm (diameter).

Non-isothermal sintering experiments were done at a heating rate of 120°C h^{-1} to 1200°C, immediately followed by cooling with a rate of 240°C h^{-1}. Isothermal experiments were done at 1050°C for 5 h and at 1070 and 1150°C for 10 h (heating rate 120° h^{-1}, cooling rate 240°C h^{-1}).

2.3 Characterization techniques

A PL Thermal Sciences system (STA 625) was used for thermogravimetric and differential thermal analysis (TGA/DTA) (in air, heating rate 600°C h^{-1}). Nitrogen sorption isotherms were obtained at 77 K using a Micromeretics ASAP 2400 system. Specific surface areas were calculated by the BET method; no corrections for microporosity were necessary. Mesopore size distributions were calculated from the adsorption branch assuming cylindrical pore shape. The phase composition was analysed by X-ray diffraction (XRD) using a Philips PW 1370 diffractometer with Cu K_α radiation. Peaks were corrected for the $K_{\alpha1}/K_{\alpha2}$ doublet and instrumental broadening. Crystallite sizes of the powders were determined by X-ray line broadening assuming Cauchy line profiles. Grain sizes in sintered specimens were determined by the lineal intercept technique from scanning electron micrographs (Hitachi S800) of polished, thermally etched cuts using $D = 1{\cdot}56\ L$, where L is the average lineal intercept.[19] Corrections for residual porosity were made by the method proposed by Wurts and Nelson.[20] The surfaces of specimens for examination by scanning electron microscopy (SEM) were coated with Au/Pd to prevent charging.

3 Results

3.1 Powder characteristics

Phase analysis by XRD revealed that all powders are tetragonal with only traces of monoclinic zirconia. The primary crystallite size as calculated from X-ray line broadening data (XRLB) of the AC500, HC-W, HC-W400 and HC-E400 powders is ~8 nm, while that of the MC-SD400 and MC-E400 powders is ~5 nm.

DTA/TGA analyses were performed in air up to 800°C for all powders before heat treatment or calcination. The DTA pattern of the AC powder showed three peaks at 300, 430 and 475°C. The first two peaks are related to the oxidative decomposition of ethoxy groups; the peak at 475°C coincides with the crystallization temperature of zirconia.[11,12,15] The total weight loss of this material upon heating is 25%. The DTA pattern for HC-W material did not show any peaks. The weight loss of this material upon heating was only 4%. The DTA pattern of the HC-E powder showed two peaks at 310 and 380°C. The TGA pattern of the HC-E powder shows a distinct decrease in weight of ~1·5% between 300 and 400°C. Both peaks observed in the DTA pattern are therefore likely to be related to the oxidative decomposition of chemisorbed ethoxy groups. The total weight loss of the HC-E material upon heating is 5%. The MC-SD material shows two peaks in the DTA pattern at 310 and 420°C. These peaks correspond to a strong weight loss and are probably related to adsorbed methanol groups. The total weight loss of the material upon heating is 14%. The DTA pattern of the MC-E powder showed only a single peak at 420°C; weight loss upon heating for this material is 16%.

As a consequence of the DTA results, the AC powder was calcined at 500°C (AC500) to make sure that all powder crystallized. The HC-E powder was treated at 400°C (HC-E400) in order to eliminate the chemisorbed ethoxy groups. The MC-SD and MC-E powders were both treated at 400°C. DTA measurements performed after these heat treatments indicated that the powders were free of chemisorbed species and were fully crystalline.

The specific surface area of the powders is dependent on the crystallization medium. Crystallization in methanol (samples MC-E400 and MC-SD400) results in the largest surface area and the smallest average crystallite size, as shown in Table 2. After heat treatment at 400°C, the specific surface areas of both HC-E400 and HC-W400 are equal (91 $m^2\ g^{-1}$).

Assuming that the volume V_p of the pores measured by N_2 adsorption/desorption can be ascribed to (intra)-agglomerate porosity, the porosity P was calculated using.[7]

$$P = \frac{V_p \rho_{th}}{(V_p \rho_{th} + 1)} \quad (1)$$

Table 2. Powder and agglomerate properties of the powders investigated [S_{BET} is specific surface area; P is agglomerate porosity; P_y is yield point; m is constant from eqn (2)]

Material code	*Crystallite size (nm)*	S_{BET} *($m^2 g^{-1}$)*	P*(%)*	P_y *(MPa)*	m	*Modus pore size (nm)*
AC500	8	103	73	80	14	9·5
HC-W	8	117	56	62	8	6·5
HC-W400	8	91	56	130	7	9·5
HC-E400	8	91	67	64	11	9·5
MC-SD400	5	144	77	41	11	6·5
MC-E400	5	144	77	55	12	6·5

where ρ_{th} is the theoretical density (6.06 g cm^{-3}). In Table 2, it can be seen that the agglomerate porosities are in the range 56 to 77% for all powders. These results indicate that the agglomerate porosity is dependent on both crystallization medium (air, water or methanol) and washing liquid used before final heat treatment. The largest porosities (77%) are obtained for methanol crystallized materials (MC); the supercritical drying after treatment (MC-SD400) did not affect the final porosity.

3.2 Compaction behaviour

The relative density of the powders as a function of the logarithm of isostatic compaction pressure is given in Fig. 1. The curves show two linear parts (parts 1 and 2) with a point of intersection at pressure P_y. Below P_y, the increase in density is rather low.

According to Van de Graaf *et al.*,[21] the intersection P_y is a measure of the strength of the agglomerates. After compaction at a pressure around P_y, the agglomerates are gradually fragmented, while they are only rearranged at pressures below P_y. Above P_y, rearrangement of the internal agglomerate structure takes place. This part of the compaction curve (part 2) can be described by the empirical equation.[7,12,22,23]

$$\rho - \rho_y = m \times \ln [P/P_y] \quad (2)$$

where m is a constant, ρ the density and P the pressure. The subscript y stands for yield point. The values of P_y and m are given in Table 2. The P_y values of the HC-W and the AC500 powder are 62 and 80 MPa, respectively. Because the HC-W powder shows a lower agglomerate porosity and the same crystallite size, the lower P_y value for the HC-W powder can be related to weaker intercrystalline bonds in the HC-W powder than in the AC500 powder. This is in accordance with results reported by Haberko and Pyda,[13] who studied hydrothermal crystallization of ZrO_2–CaO.

If HC-W and HC-W400 are compared it is clear that the heat treatment at 400°C results in a strengthening of the intercrystalline bonds, because agglomerate porosity and crystallite size remain the same while P_y increases. The influence of washing medium used after hydrothermal crystallization on agglomerate strength is demonstrated by the powders HC-W400 and HC-E400, which have an agglomerate strength of 130 and 64 MPa, respectively. The smaller agglomerate strength of HC-E400 is, in this case, probably related to the larger agglomerate porosity and/or a difference in strength of the intercrystalline bonds. The slightly higher agglomerate strength of the HC-E400 material compared with the MC-E400 material is probably related to the smaller agglomerate porosity of the former. The agglomerate strength of the MC-SD400 material (P_y = 41 MPa) is smaller than of the MC-E400 material (P_y = 55 MPa). This shows the influence of supercritical drying in this case.

A large value of m (the slope of the high pressure curve) corresponds to a relatively rapid increase in relative density with compaction pressure. A large value of m might be an indication of a large

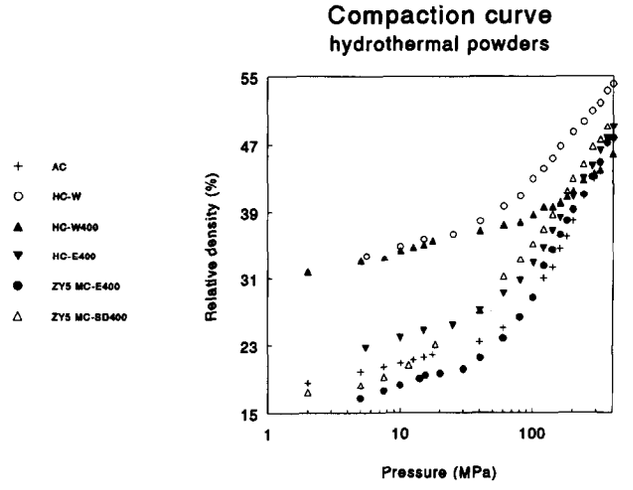

Fig. 1. Densification behaviour of the ZY5 powders during isostatic compaction.

density distribution in the green compact. Some sources of density variations are the friction between the powder and the die wall and between the powder particles. The specimen may fracture during unloading or ejecting of the pressed part, especially when large specimens are made. The m values of the various powders range between 7 and 14, as can be seen in Table 2. It is expected that the stresses created during compaction of the HC-W and HC-W400 material are small, therefore it should be easy to prepare large samples of this material.

3.3 Green compact properties

Figure 2 shows adsorption/desorption isotherms of green compacts (pressed at 400 MPa). The shape of the hysteresis loop is an indication of the pore morphology. The hysteresis of the HC-W and MC-SD400 materials is predominantly of type E, following the classification of De Boer.[24] The AC500 material is of a mixed type A/E, while the MC-E400 and HC-E400 (≈HC-W400) materials are in between (curves of the HC-W400 and MC-E400 materials are not shown here). Type E is indicative of tubular capillaries with strongly varying widths (as expected in powder compacts), while type A corresponds to a cylindrical pore shape. During sintering of a AC500 powder compact, the hysteresis shape becomes more and more similar to type A due to progressive neck formation.[25] The differences in green porous texture between the powders are most probably caused by partial sintering already taking place during crystallization in air (500°C) or heat treatment (400°C) after crystallization in water or methanol of the normal dried powder, while partial sintering does not take place when the hydrothermally crystallized powder is only filtered and dried at 120°C (HC-W). Neck formation during heat treatment is reduced in the case of supercritical drying

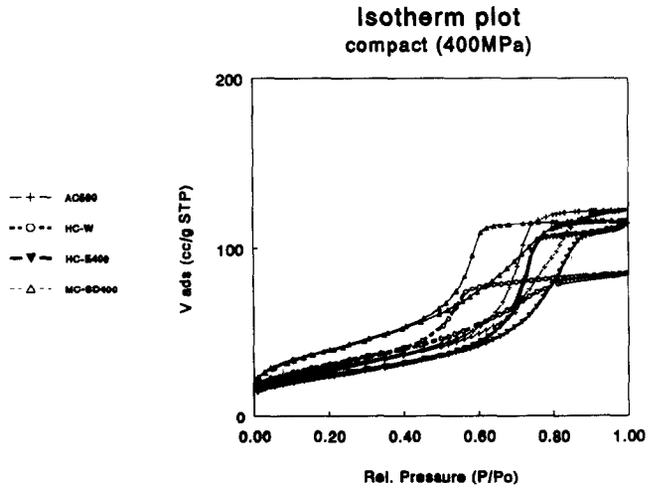

Fig. 2. N_2 sorption isotherms of green compacts.

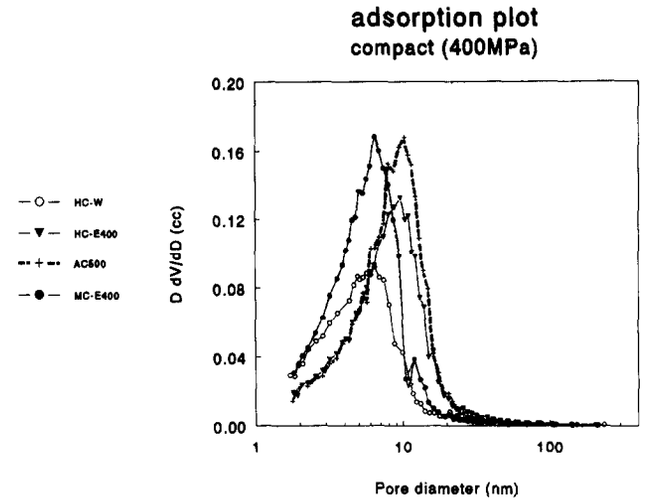

Fig. 3. Pore size distributions in the powder compacts after isostatic pressing at 400 MPa.

(MC-SD400), resulting in an E type hysteresis and low P_y values.

The pore size distributions of green compacts are given in Fig. 3. The width of the pore size distribution is similar for all powders, with the exception of the HC-W powder, which has a slightly broader distribution. The most frequently found pore diameter of the HC-E400, HC-W400 and AC500 compacts is the same and equals 9.5 nm, whereas the HC-W, MC-SD400 and MC-E400 materials have a maximum at 6.5 nm. Since the crystallite sizes of the AC500, HC-W, HC-W400 and HC-E400 materials are the same, the smaller average pore diameter of the HC-W green compact results from improved compactability resulting in a better particle stacking.

3.4 Sinterability and microstructure

The increase in relative density with temperature was measured using a heating rate of 120°C h^{-1} to 1200°C. The results for the AC500, HC-W, HC-W400 and MC-SD400 materials can be seen in Fig. 4.

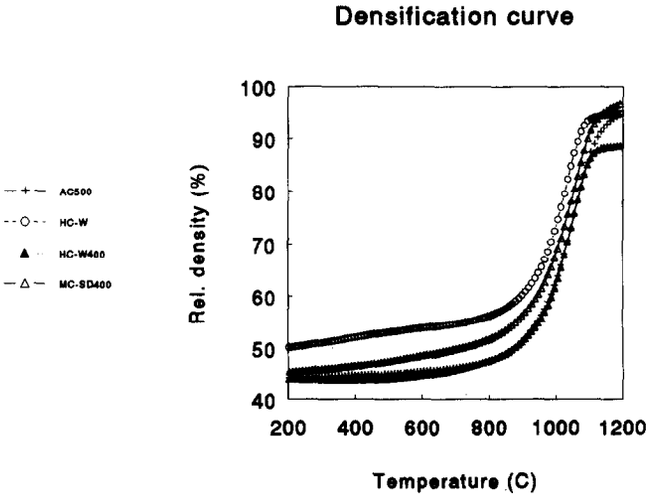

Fig. 4. Increase of relative density with temperature during heating at 120°C h^{-1}.

The HC-E400 and MC-E400 materials show approximately the same densification behaviour as the AC500 material. The maximum in densification rate is found at a temperature of around 1040°C for all cases. The HC-W400 material has the lowest final density (90%), probably due to the harder agglomerates present in the powder. The other materials show only small differences in sinterability, these samples being 95% dense at 1150°C. From the non-isothermal sintering behaviour, it is evident that it should be possible to sinter the five systems to full density at a temperature below 1100°C. For the AC500, HC-W, HC-E400, MC-E400 and MC-SD400 materials, isothermal sintering experiments were performed at 1050°C. The increase in relative density with time during sintering at 1050°C is illustrated in Fig. 5. The AC500 material is 90% dense and the HC-E400, MC-E400 and MC-SD400 materials are 93, 93 and 94% dense, respectively, after 5 h of sintering. The HC-W material is 94% dense after 2 h of sintering at this low temperature. The average grain size of the materials after sintering at 1050°C/5 h is between 95 and 100 nm in all cases. The microstructure is homogeneous, as is shown for the HC-E400 material in Fig. 6. HC-E400 and MC-SD400 were also sintered at 1150°C for 10 h, resulting in a density of 98% and a grain size of 180 nm. Sintering the AC500 and HC-E400 materials at 1070°C for 10 h resulted in a grain size between 120 and 130 nm and a relative density of 93 and 96% for AC500 and HC-E400, respectively. In the HC-W material, small cracks were observed by SEM, as is shown in Fig. 7. No cracking was observed for the other materials. A drawback of the AC500 material is that it results in irreproducible final densities. After sintering for 10 h at 1150°C, densities varied between 92 and 97%. The densification

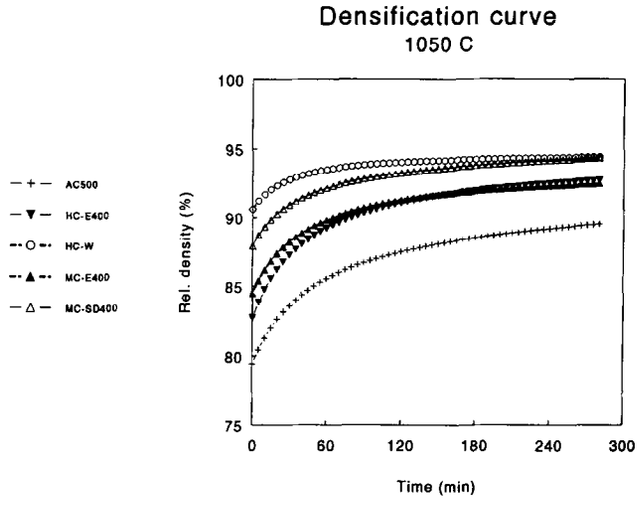

Fig. 5. Increase of relative density with time during sintering at 1050°C.

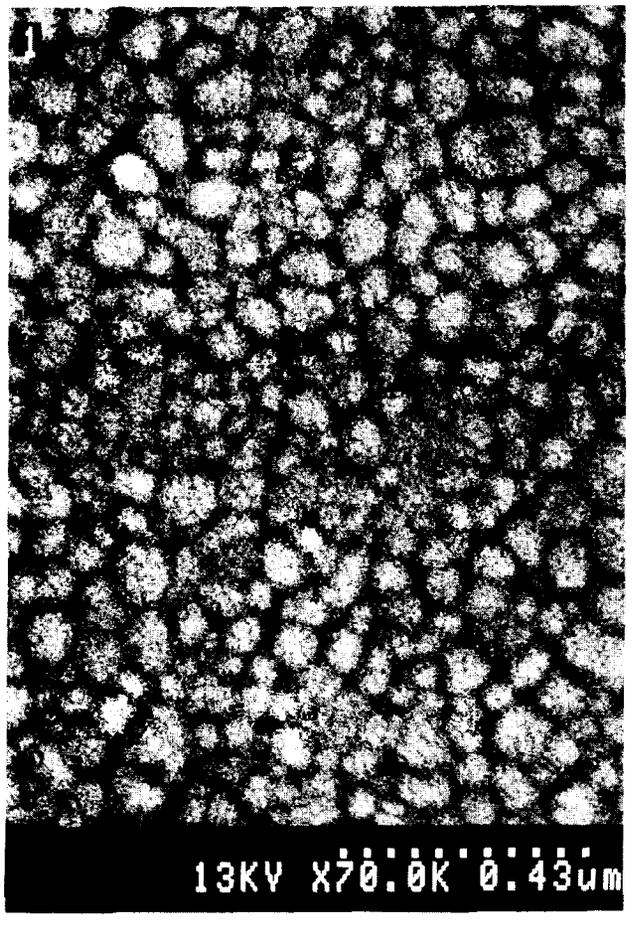

Fig. 6. Microstructure of the HC-E400 material sintered for 5 h at 1050°C.

Fig. 7. Microstructure of the HC-W material sintered at 1050°C for 5 h showing a crack.

characteristics of the hydrothermal powders are very reproducible.

4 Discussion

4.1 The effect of liquid medium before final heat treatment on powder properties

Final heat treatment of hydrothermal powder results in a larger pore size and smaller pore size distribution. The neck area is also increased by this heat treatment. Boutz *et al.*[25] observed that an increase in heat treatment temperature of an air-crystallized powder compact (starting at 500°C) leads to an increase in pore size, narrowing of the pore size distribution and increase in neck area. The results observed for the HC-W and HC-W400 materials indicate that the same holds for hydrothermally crystallized powders for temperatures down to 200°C (hydrothermal crystallization temperature). After hydrothermal crystallization, the liquid medium does not influence the pore size, pore size distribution or the pore shape. Materials HC-W400 and HC-E400 show identical results.

The agglomerate strength of air-crystallized powder can be reduced if water is replaced by ethanol before crystallization. This reduction is extremely large. It was found that the agglomerate strength of a water-washed air-crystallized powder is >400 MPa, whereas the agglomerate strength of ethanol-washed air-crystallized powder varies between 60 and 90 MPa. This reduction in strength has been ascribed to the formation of ethoxide groups on the surface[8] and to the lower compaction pressure during drying due to the lower surface tension of ethanol compared with water.[9,10] In the case of hydrothermally crystallized powder, the agglomerate strength is reduced to a lesser extent if water is replaced by ethanol after crystallization: 130 MPa for HC-W400 compared with 64 MPa for HC-E400 powder. This means that the effect of the washing medium can be reduced by crystallization before final heat treatment. However, this influence cannot be neglected yet. The reduction in agglomerate strength is likely to result from the increase in agglomerate porosity. The increase of agglomerate strength with heat treatment temperature (HC-W and HC-W400) is caused by an increase in neck area.

The hydrothermally crystallized powders show good sintering characteristics. The observed cracking of the HC-W material might be related to stresses forming in the temperature range 200–700°C during densification of agglomerates containing a large number of pores with a diameter <6 nm. Cracking of the HC-W material can be avoided if a lower heating rate is used until 700°C.

4.2 The effect of crystallization medium on powder properties

A comparison will be made between crystallization in air, water and methanol. Crystallization in methanol results in a smaller crystallite size than is obtained by hydrothermal crystallization or crystallization in air. The difference in pore size between AC500 and HC-E400 on one hand, and MC-E400 on the other hand might be caused by this difference in crystallite size.

More neck area is obtained by crystallization in air than by crystallization in liquid media. This might be caused by the higher crystallization temperature. To a large extent, the strength of the intercrystalline bonds and agglomerate porosity determine the agglomerate strength of the material.[5] It is reasonable to assume that the strength of the intercrystalline bonds is increased if the neck area is increased. Therefore, the agglomerate strength of the methanol-crystallized material is expected to be the smallest; this is in agreement with experimental results (as indicated by P_y values).

The sinterability of the material is not influenced by the crystallization medium. The low reproducibility of achieving high final densities of the air-calcined material can have several causes. Some of these are: a large agglomerate-strength distribution; the irregular agglomerate shape; and the large differences in agglomerate sizes in the powder. The synthesis of Y-TZP with reproducible high final densities from air-crystallized material is still under investigation.

4.3 The effect of supercritical drying of methanol-crystallized material on powder properties

The effect of supercritical drying on powder properties has been analysed for methanol-crystallized material. The results obtained for the methanol-crystallized materials show that supercritical drying has no influence on pore size, pore size distribution, agglomerate porosity or sinterability of the material. Supercritical drying does, however, result in less neck area compared with normal drying which, with the same agglomerate porosity, leads to a smaller agglomerate strength. This will lead to a more homogeneous microstructure in the green and sintered compact.

5 Conclusions

(1) Pressureless sintering of the hydrothermally or methanol-crystallized material that was ethanol-washed and subsequently heat-treated, results in relatively dense (93–94%), nanostructured (<100 nm) Y-TZP at a sintering temperature as low as 1050°C.

(2) Densities can be increased to 96% at 1070°C and 98% at 1150°C, with resulting grain sizes of 130 and 180 nm, respectively.
(3) The as-dried hydrothermally crystallized material (HC-W) exhibited small cracks after sintering, probably caused by stresses associated with the densification of agglomerates. Cracking can be avoided by low heating rates up to 700°C.
(4) The effects of supercritical drying after crystallization in methanol are minor.
(5) The powder characteristics, compactability, green compact properties and sinterability of the air-calcined and hydrothermally crystallized materials that were ethanol-washed and heat-treated, are almost the same.
(6) Crystallization in methanol instead of water or air results in smaller crystallites and softer agglomerates.
(7) Replacing water by ethanol directly after hydrothermal crystallization results in an increase in agglomerate porosity.

Acknowledgements

These investigations were partly supported by the Innovative Research Program on Technical Ceramics (IOP-TK) with financial aid from the Dutch Ministry of Economic Affairs.

References

1. Burggraaf, A. J., Stuijts Memorial Lecture 1991: Some new developments in ceramic science and technology. *J. Eur. Ceram. Soc.*, **9** (1992) 245–50.
2. Burggraaf, A. J., Winnubst, A. J. A. & Verweij, H., Dense and porous nanostructured ceramics and composites. In *Proceedings of the Third Meeting of the European Ceramic Society*, ed. P. Duran & J. F. Fernandez. Faenza Editrice Iberica, 12–17 1993, pp. 561–76.
3. He, Y. J., Winnubst, A. J. A., Burggraaf, A. J., Verweij, H., van der Varst, P. G. Th. & De With, B. G., Grain size dependence of sliding wear in tetragonal zirconia polycrystallines. Submitted to *J. Am. Ceram. Soc.*
4. Theunissen, G. S. A. M., Microstructure, fracture toughness and strength of (ultra)fine-grained tetragonal zirconia ceramics. PhD thesis, University of Twente, Enschede, The Netherlands, 1991, Ch. 7.
5. Rumf, H., Grundlagen und Methoden des Granulierens. *Chemie Ing. Techn.*, **30** (1958) 144–58.
6. Haberko, K., Characteristics and sintering behavior of zirconia ultrafine powders. *Ceramurgia Int.*, **5** (1979) 145–58.
7. Groot Zevert, W. F. M., Winnubst, A. J. A., Theunissen, G. S. A. M., & Burggraaf, A. J., Powder preparation and compaction behaviour of fine-grained Y-TZP. *J. Mater. Sci.*, **25** (1990) 3449–55.
8. Kaliszewski, M. S. & Heuer, A. H., Alcohol interaction with zirconia powder. *J. Am. Ceram. Soc.*, **73** (1990) 1504–9.
9. Roosen, A. & Hausner, H., The influence of processing conditions on the sintering behaviour of coprecipitated calcia-stabilized zirconia powders. In *Ceramic Powders* (Materials Science Monographs 16), ed. P. Vincenzini. Elsevier, Amsterdam, 1983, pp. 773–82.
10. Dogan, F. & Hausner, H., The role of freeze-drying in ceramic powder processing. In *Ceramic Trans., Ceramic Powder Science (II)*, Vol. 1, ed. G. L. Messing, E. R. Fuller Jr & H. Hausner. American Ceramics Society, Westerville, OH, 1988, pp. 127–34.
11. Mercera, P. D. L., Van Ommen, J. G., Doesburg, E. B. M., Burggraaf, A. J. & Ross, J. R. H., *J. Mater. Sci.*, **27** (1992) 4890.
12. Theunissen, G. S. A. M., Microstructure, fracture toughness and strength of (ultra)fine-grained tetragonal zirconia ceramics. PhD thesis, University of Twente, Enschede, The Netherlands, 1991, Ch. 2.
13. Haberko, K. & Pyda, W., Preparation of Ca-stabilized ZrO_2 micropowders by a hydrothermal method. In *Advances in Ceramics*, vol. 12, American Ceramics Society, Westerville, OH, 1984, p. 774–83.
14. Pyda, W., Haberko, K. & Bucko, M. M., Hydrothermal crystallization of zirconia and zirconia solid solutions. *J. Am. Ceram. Soc.*, **74** (1991) 2622–9.
15. Boutz, M. M. R., Olde Scholtenhuis, R. J. M., Winnubst, A. J. A. & Burggraaf, A. J., A hydrothermal route for production of dense, nanostructured Y-TZP. *Mater. Res. Bull.*, **29** (1994) 31–40.
16. Rossi, G. A. & Pelletier, P. J., Y_2O_3 doped ZRO_2 powder prepared in nonaqueous medium. Influence of the crystallization method on powder sinterability and properties of Y-TZP ceramics. In *Advances in Ceramics, Vol. 24: Science and Technology of Zirconia III*, ed. S. Somiya, N. Yamamoto & H. Yanagida. American Ceramics Society, Westerville, OH, 1988, pp. 173–81.
17. Sato, T., Dosaka, K., Yoshioka, T., Okuwaki, A., Torii, K. & Onodera, Y., Sintering of ceria doped tetragonal zirconia crystallized in organic solvents, water, and air. *J. Am. Ceram. Soc.*, **75** (1992) 552–6.
18. Henderson, J. B., Emmerich, W.-D. & Wassmer, E., A method for the temperature calibration of pushrod dilatometers. *J. Thermal Anal.*, **32** (1987) 1905–13.
19. Mendelson, M. I., Average grain size in polycrystalline ceramics. *J. Am. Ceram. Soc.*, **52** (1969) 443–6.
20. Wurts, J. C. & Nelson, J. A., Lineal intercept technique for measuring grain size in two-phase polycrystalline ceramics. *J. Am. Ceram. Soc.*, **55** (1972) 109.
21. Van de Graaf, M. A. C. G., Ter Maat, J. H. H. & Burggraaf, A. J., Microstructure and sintering kinetics of highly reactive ZrO_2–Y_2O_3 ceramics. *J. Mater. Sci.*, **20** (1985) 1407–18.
22. Halloran, J. W., Role of powder agglomerates in ceramic processing. In *Advances in Ceramics*, Vol. 9, ed. J. A. Mangels & G. L. Messing. American Ceramics Society, Inc., Columbus, OH, 1984, pp. 67–75.
23. Halloran, J. W., Agglomerates and agglomeration in ceramic processing. In *Ultrastructure Processing of Ceramics, Glasses and Composites*, ed. L. L. Hench & D. R. Ulrich. John Wiley and Sons, New York, 1984, pp. 404–17.
24. De Boer, J. H., *The Structure and Properties of Porous Materials*. Butterworth Scientific Publications, 1958, pp. 68–93.
25. Boutz, M. M. R., Winnubst, A. J. A. & Burggraaf, A. J., Yttria-ceria stabilized tetragonal zirconia polycrystals sintering, grain growth and grain boundary segregation. *J. Eur. Ceram. Soc.*, **13** (1994) 89–102.